Electronic Supplementary Material (ESI) for ChemComm.

Photocatalytic CO_2 reduction using visible light by a metal-monocatecholato species in a metal-organic framework

Yeob Lee,[a] Sangjun Kim,[b] Honghan Fei,[a] Jeung Ku Kang*[bc] and Seth M. Cohen*[a]

[a]*Department of Chemistry and Biochemistry, University of California, San Diego, 9500 Gilman Drive, La Jolla, California, United States 92093-0358,*

[b]*Department of Materials Science and Engineering,*

[c]*Graduate School of EEWS, KAIST, 291 Daehakro, Yuseonggu, Daejeon, Republic of Korea 305-701.*

Supporting Information

* To whom correspondence should be addressed. E-mail: jeung@kaist.ac.kr; scohen@ucsd.edu. Telephone: +1 (858)822-5596

Experimental

Synthesis of UiO-66-CAT. UiO-66-CAT was synthesized by PSE following a previously reported procedure.[S1] Pristine UiO-66 was prepared using solvothermal methods from $ZrCl_4$ (Alfa Aeser, 16 mg, 0.07 mmol), H_2bdc (benzene-1,4'-dicarboxylic acid, Aldrich, 11.6 mg, 0.07 mmol), and acetic acid (Alfa, 210 mg, 3.5 mmol) dissolved, with the aid of sonication, in 4 mL of DMF in a scintillation vial. The vial was then transferred to a preheated isothermal oven at 120 °C for 24 h. After cooling, the mixture was collected by centrifugation, and the resulting white powders were soaked in MeOH for 3 d, with the solution was replaced with fresh MeOH (10 mL) every 24 h. After 3 d of soaking, the solids were isolated via centrifugation, followed by drying under vacuum at room temperature. To achieve PSE, the H_2catbdc ligand[S2] (0.2 mmol) was dissolved in 2 mL of 4% KOH solution with sonication, followed by neutralization of the solution with a minimal amount of 1M HCl to pH = 7. Another 0.5 mL of DMF was added to the mixture to obtain a H_2O/DMF solution containing $catbdc^{2-}$. Pristine UiO-66 (28 mg, 0.1 mmol, ~0.1 eq. based on bdc) was introduced into the $catbdc^{2-}$ solution, followed by incubation of the mixture in a preheated isothermal oven at 85 °C for 48 h. After cooling, the mixture was centrifuged, and washed thoroughly with 10 mL of MeOH five times. The pale-brown powders were soaked in MeOH for 3 d, and the solution was replaced with fresh MeOH (10 mL) every 24 h. After 3 d of soaking, the solid was isolated via centrifugation and then dried under vacuum at room temperature. This produced UiO-66-CAT where ~34% of the bdc^{2-} linkers had been replaced by $catbdc^{2-}$, which was used for the remaining studies reported here.

Metalation of UiO-66-CAT with Cr(III). K_2CrO_4 (Aldrich, 16 mg, 0.08 mmol Cr) was dissolved in 2 mL deionized water. The pH of the solution was adjusted to ~3 with a minimal amount of 1 M HCl. UiO-66-CAT (31 mg, 0.1 mmol, ~0.1 equiv based on the

organic linkers, 34% catbdc after PSE, see above) was placed into the K_2CrO_4 solution. The MOF particles were dispersed using sonication, followed by incubation at room temperature. After 1 h, the dark-brown powder was collected via centrifugation and washed with both deionized water (3×10 mL) and MeOH (3×10 mL). The solids were soaked in MeOH for 3 d, and the solution was replaced with fresh MeOH every 24 h. After 3 d of soaking, the solids were isolated via centrifugation and dried under vacuum at room temperature. Inductively coupled plasma mass spectrometry (ICP-MS, Table S1) indicated that 76±2% of the available catbdc ligands were metalated by Cr using this procedure (based on three independent samples).

Metalation of UiO-66-CAT with Ga(III). $Ga(NO_3)_3(H_2O)_x$ (Aldrich, 24 mg, 0.08 mmol Ga) was dissolved in 2 mL deionized water. UiO-66-CAT (31 mg, 0.1 mmol, ~0.1 equiv based on the organic linkers, 34% catbdc after PSE, see above) was placed into the $Ga(NO_3)_3(H_2O)_x$ solution. The MOF particles were dispersed using sonication, followed by incubation in a preheated isothermal oven at 55 °C overnight. After cooling, the pale-brown powder was collected via centrifugation and washed with both deionized water (3×10 mL) and MeOH (3×10 mL). The solids were soaked in MeOH for 3 d, and the solution was replaced with fresh MeOH every 24 h. After 3 d of soaking, the solids were isolated via centrifugation and then dried under vacuum at room temperature. ICP-MS (Table S1) indicated that 77±3% of the available catbdc ligands were metalated by Cr using this procedure (based on three independent samples).

Powder X-ray Diffraction (PXRD) analysis. PXRD patterns were collected on a Bruker D8 Advance diffractometer. 20-30 mg of MOF samples were loaded on glass holder and measured at 40 kV, 40 mA for Cu Kα (λ=1.5418 Å), with a scan speed of 2 deg/min in

2θ, and a 2θ range of 5° to 40°.

Scanning Electron Microscopy (SEM) and Energy-dispersed X-ray spectroscopy (EDX). SEM images were collected on a Phillips XL 30 ESEM instrument. 2-3 mg of MOFs were dispersed on carbon tape and sputtered with iridium for conductivity. The SEM was operated at 10 kV of acceleration voltage with spot size of 3. Oxford EDX and Inca software were used to perform elemental analysis using characteristic X-rays for each element of interest.

Diffuse Reflectance UV-Vis Spectroscopy. UV-Vis spectra were collected using a StellarNet, EPP 2000C spectrophotometer with a diffuse reflectance measurement system. A step size of 1 nm/sec and a wavelength range of 300 nm to 800 nm were used. F(R) values were calculated by Kubelka-Munk function of $(1-R)^2/2R$ for solid state samples. A polytetrafluoroethylene (PTFE) disk (StellarNet, RS-50), which reflects >97% of incident light (300 nm < λ < 1700 nm), was used as a reference (R).

Inductively Coupled Plasma Mass Spectrometer (ICP-MS) analysis. ICP-MS was used to determine the metal content of Zr, Cr, and Ga in MOF samples. ICP-MS analysis was performed on an Agilent ICP-MS 7700S. MOF samples were dissolved in 7:3 (v/v) solution of HNO_3-HCl and thermally treated at 200 °C with the aid of a microwave reactor prior to analysis.

Photoluminescence (PL) Analysis. Light emission properties of MOFs were recorded on a Horiba LabRam HR PL photoluminescence spectrometer using a 325 nm laser as the excitation source. 2-3 mg of samples were placed in a hole at the center of a plate-

type cell, then MOFs were exposed to laser source. All parameters were same for precise comparison between Zr-based MOFs and metalated MOFs.

Lifetime of Solid-state Fluorescence Analysis. Lifetimes of solid-state fluorescence for MOFs were obtained by a time-correlated single photon counting (TCSPC) method using an Edinburgh Instruments FL920 spectrofluorometer equipped with 375 nm laser for excitation light source. A detection wavelength of 550 nm was used for all MOF samples.

pH Measurements. pH of photocatalysis solutions were measured using a Thermo Scientific Origon 3-starpH meter equipped with glass body combination electrode. The pH meter was calibrated by two points method using aqueous buffers of pH 4.01 (Orion pH buffer 910104) and pH 10.01 (Orion pH buffer 910110).

Photocatalytic CO_2 Reduction Experiments. 5 mg of photocatalyst was dispersed in 5 mL of 4:1 (v/v) mixed solution of acetonitrile (MeCN)-triethanolamine (TEOA), which contained 1-benzyl-1,4-dihydronicotiamide (0.1 M, BNAH). The suspension was purged by CO_2 gas at a pressure of 1 bar for 30 min. The resulting solution was placed under visible light irradiation using a 300 W Xe arc lamp (Newport, 6258) with power supply (Newport, 66983) equipped with two cut-off filters to ensure visible light irradiation (420 nm < λ < 800 nm). Cooling water circulation for heat dissipation was applied. The visible light was irradiated to the reactor with 5 cm of distance and the intensity of incident light was 100 mW/cm^2 (measured by a radiometer (FieldMaxII equipped with PowerMax, Coherent)). The reaction products, including formic acid, were extracted following reported procedure.[S3] After 6 h of photocatalysis, the suspension was subjected to centrifugation at 7000 rpm for 15 min using a Hettich Rotana 460R centrifuge equipped with as A5615 fixed-angle rotor to

remove the photocatalyst. The products were extracted using 3 mL of ethyl acetate. The ethyl acetate solution was washed with 3 mL of 0.5 M H_2SO_4(aq) three times. 1 μL of the ethyl acetate solution containing the extracted products was injected into a GC-MS (Agilent, GC-7890A and MS-5975C) equipped with a capillary column (Supleco, 30m × 0.32mm) and MSD (Mass selective detector, inert triple-axis detector) to identify the reaction products. The initial temperature of oven was 130 °C and maintained for 5 min followed by ramping up to 230 °C at a rate of 10 °C/min. Finally, the oven was maintained at 230 °C for 25 min. CO gas was identified by a GC (Shimadzu, GC-2014A) equipped with a porus polymer column (2.1 mm diameter, 6 ft. length) using an FID (Flame Ionized Detector), and He as the carrier gas. H_2 and CH_4 gas production was characterized by a GC (Agilent, GC-7890A) equipped with a 5 Å molecular sieve column (3 mm diameter, 3 m length) and TCD (Thermal Conductivity Detector) with Ar as the carrier gas. The MOFs collected after photocatalysis (see above) were washed with MeOH (3×10 mL) and dried under vacuum at 60 °C for analysis by PXRD, ICP-MS, and for retesting for catalytic recyclability.

Liquid ^{13}C NMR of CO_2 Isotopes. ^{13}C NMR samples were prepared under the same photocatalysis reaction conditions described above section, but using a deuterated solvent and an isotope of CO_2. CD_3CN (Cambridge, 99.8% D) was used instead of CH_3CN as solvent and $^{13}CO_2$ (Aldrich, 99% ^{13}C, ~3% of ^{18}O) was used for purging gas instead of $^{12}CO_2$. After 13 h of photocatalysis, the MOFs were collected via centrifugation (as described above) and the supernatant was directly transferred to an NMR tube for analysis using a 400 MHz NMR (Agilent, 400MHz 54mm NMR DD2). $H^{13}COOH$ (Aldrich, 95 wt% in H_2O, 99% ^{13}C) was used to calibrate a chemical shift of $H^{13}COOH$ in CD_3CN and deprotonated $H^{13}COO^-$ in basic CD_3CN/TEOA solutions.

Quantum Yield Measurement. 5 mg of photocatalyst was dispersed in 5 mL of 4:1 (v/v) mixed solution of acetonitrile (MeCN)-triethanolamine (TEOA), which contained 1-benzyl-1,4-dihydronicotiamide (0.1 M, BNAH). The suspension was purged by CO_2 gas at a pressure of 1 bar for 30 min. The resulting solution was placed under visible light irradiation using a 300 W Xe arc lamp (Newport, 6258) with power supply (Newport, 66983) equipped with a band-pass filter (λ = 450 nm). Cooling water circulation for heat dissipation was applied. The reactor was irradiated with visible light at a distance of 5 cm with an intensity of 10 mW. Product treatment and analysis method is exactly same with ordinary photocatalysis tests. UiO-66-CrCAT produced 14.9±1.32 μmoles of HCOOH and UiO-66-GaCAT produced 9.53±0.95 μmoles of HCOOH, respectively.

BET Surface Area Analysis. ~50 mg of MOF samples were evacuated on a vacuum line overnight at room temperature. The samples were then transferred to a pre-weighed sample tube and degassed at 105 °C on an adsorption analyzer (Micromeritics, ASAP 2020) for a minimum of 12 h or until the outgas rate was <5 mm Hg. The sample tube was re-weighed to obtain a consistent mass for the degassed exchanged MOF. BET surface area (m^2/g) measurements were collected at 77 K by liquid N_2 on a Micromeritics ASAP 2020 Adsorption Analyzer using the volumetric technique.

References

S1. H. Fei, J. Shin, Y. S. Meng, M. Adelhardt, J. Sutter, K. Meyer and S. M. Cohen, *J. Am. Chem. Soc.*, 2014, **136**, 4965-4973.

S2. K. Raymond and J. Xu, *US Pat.*, 5 892 029, 1990.

S3. H. Takeda, H. Koizumi, K. Okamoto and O. Ishitani, *Chem. Commun.*, 2014, **50**, 1491-1493.

Supporting Figures and Tables

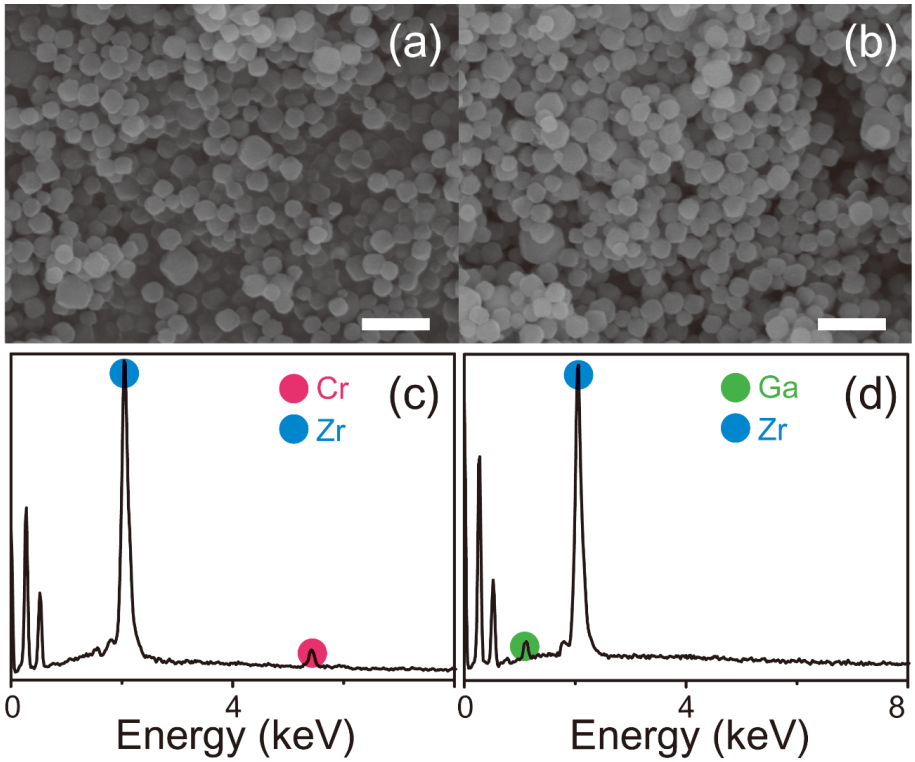

Fig. S1. Scanning electron microscopy (SEM) images of (a) UiO-66-CrCAT and (b) UiO-66-GaCAT (scale bar = 500 nm.). Energy dispersive x-ray spectroscopy of (c) UiO-66-CrCAT and (d) UiO-66-GaCAT.

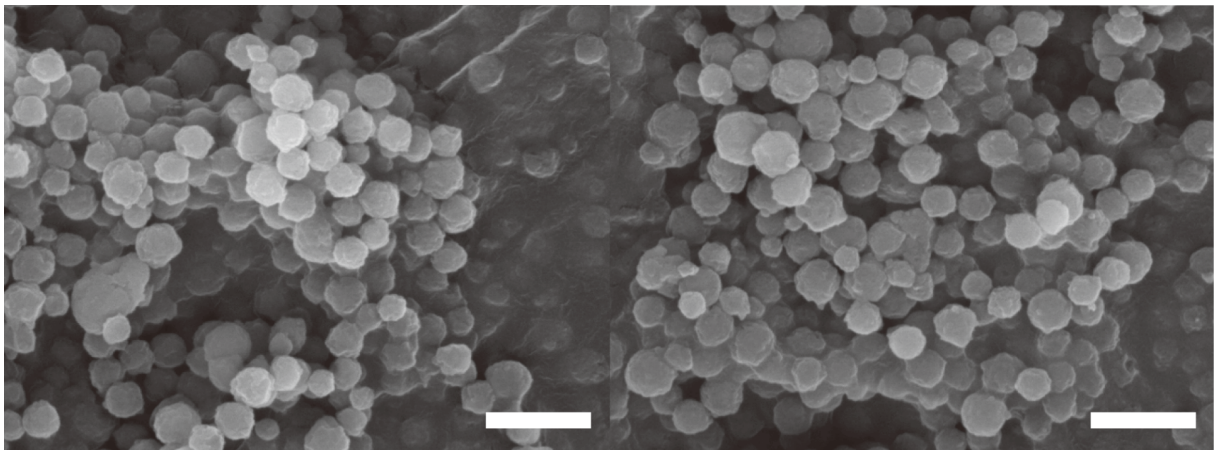

Fig. S2. Scanning electron microscopy (SEM) images of (a) UiO-66 and (b) UiO-66-CAT (scale bar = 500 nm.).

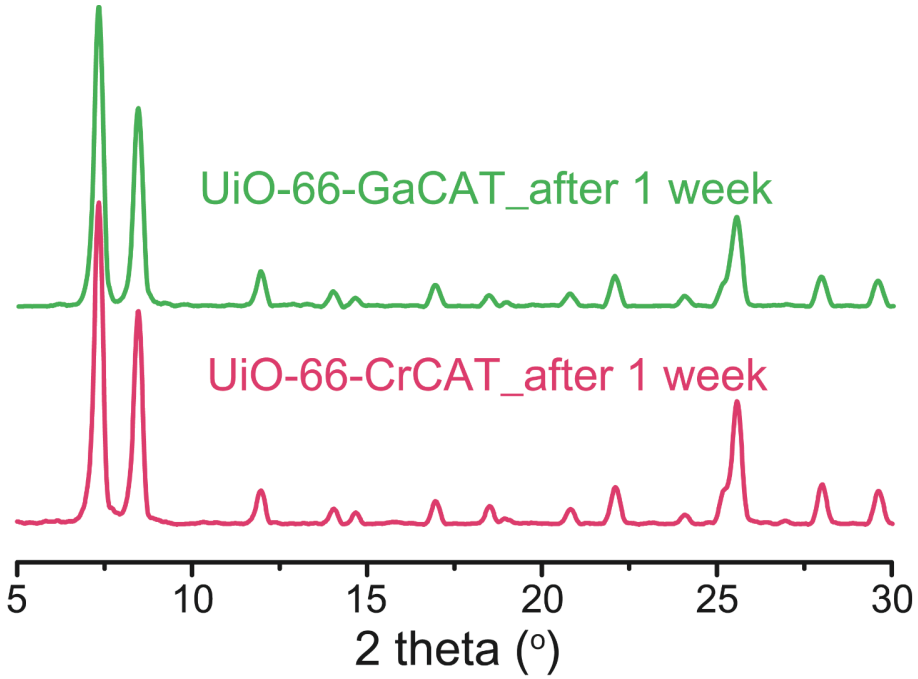

Fig. S3. PXRD patterns from UiO-66-CrCAT and UiO-66-GaCAT after soaking in 4:1 (v/v) mixed solution of MeCN and TEOA for 1 week.

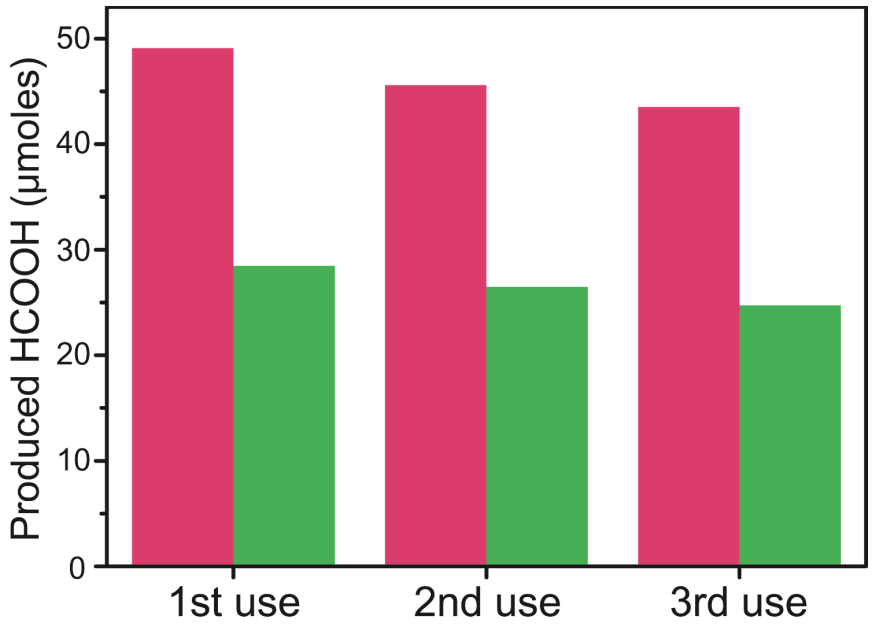

Fig. S4. Amount of HCOOH produced during photocatalysis of CO_2 over three uses of UiO-66-CrCAT (red) and UiO-66-GaCAT (green) catalysts.

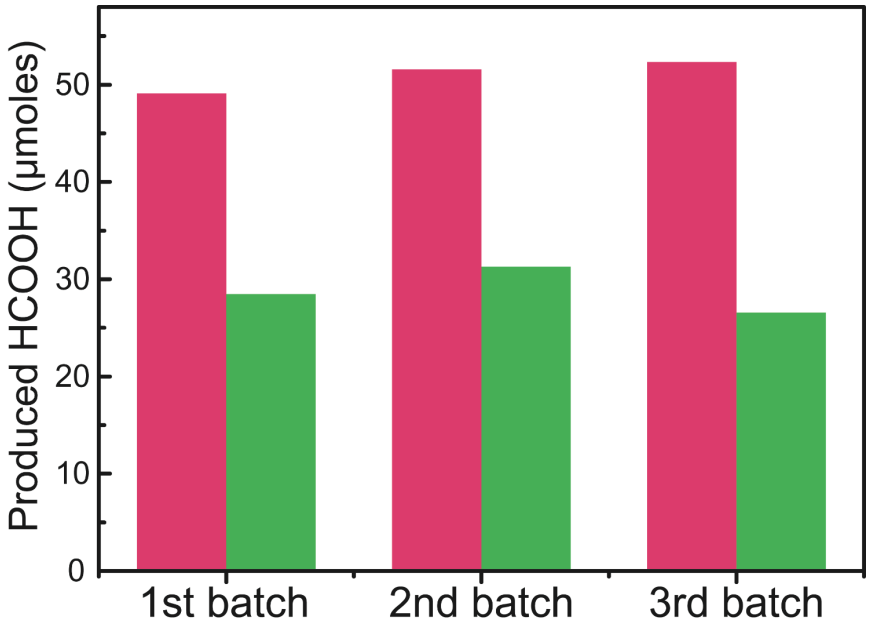

Fig. S5. Amount of HCOOH produced during photocatalysis of CO_2 using three different samples of UiO-66-CrCAT (red) and UiO-66-GaCAT (green) catalysts.

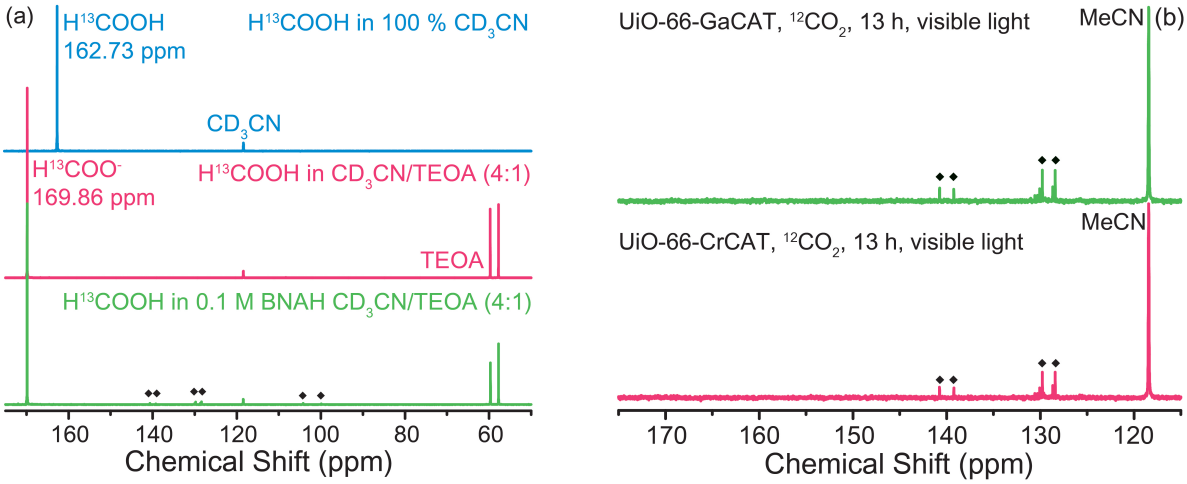

Fig. S6. *Left*: ^{13}C liquid NMR reference spectra for assigning $H^{13}COO^-$, TEOA, and BNAH resonances. $H^{13}COOH$ was found at 162.73 ppm in 100% CD_3CN, but was shifted to 169.86 ppm in an alkaline solution of 4:1 (v/v) of CD_3CN and TEOA due to deprotonation of HCOOH to $HCOO^-$. *Right*: ^{13}C liquid NMR spectra for photocatalysis products of both UiO-66-CrCAT and UiO-66-GaCAT using unlabeled $^{12}CO_2$. No $H^{13}COO^-$ peak was detected in both spectra. ◆ = BNAH.

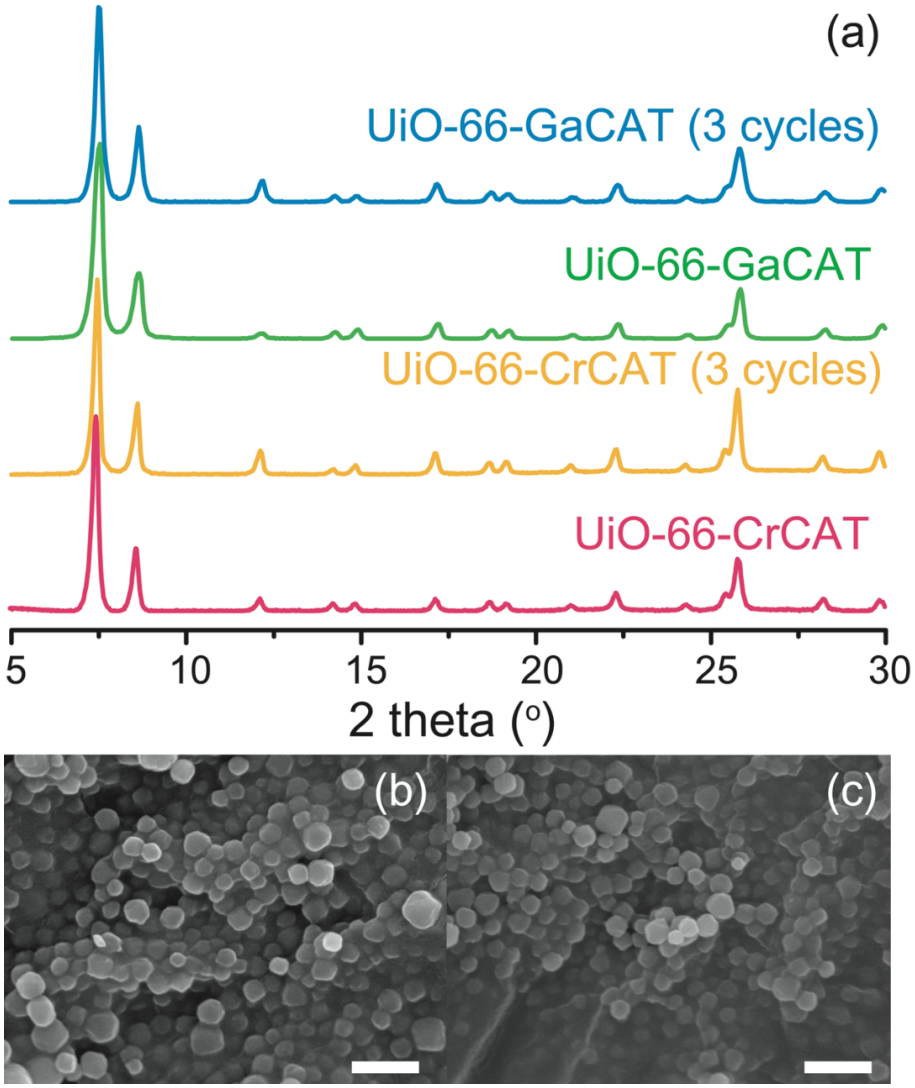

Fig. S7. (a) PXRD patterns of UiO-66-M(III)CAT MOFs after 3 cycles of photocatalysis and scanning electron microscopy images of (b) UiO-66-CrCAT and (c) UiO-66-CAT-GaCAT after 3 cycles of photocatalysis. The scale bar is 500 nm.

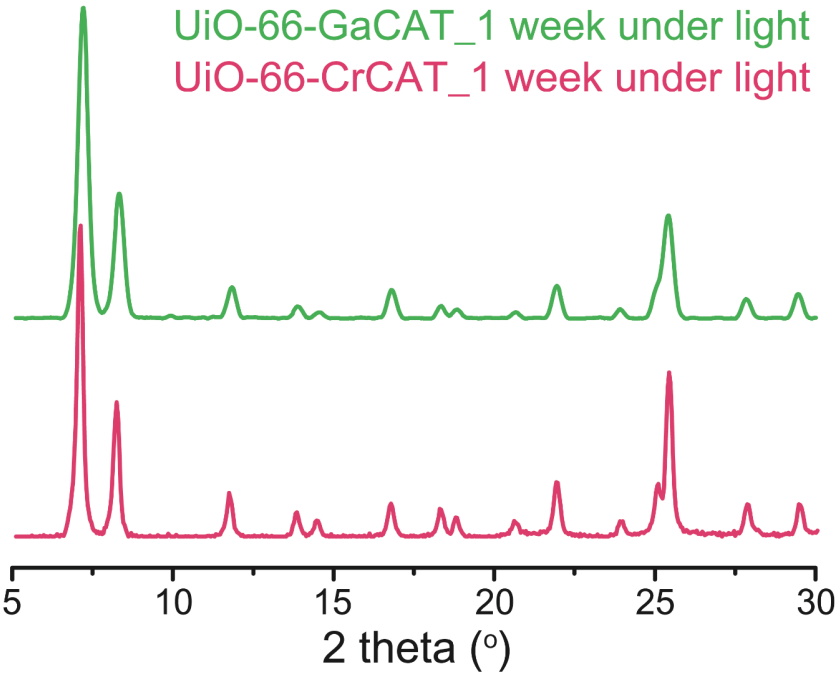

Fig. S8. PXRD patterns from UiO-66-CrCAT and UiO-66-GaCAT after light irradiation for 1 week.

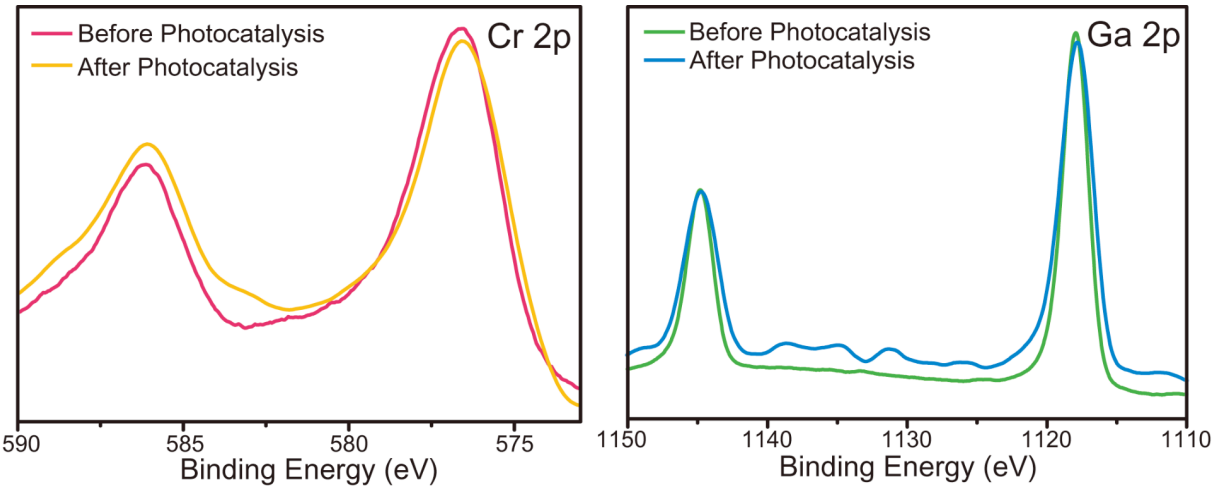

Fig. S9. X-ray photoelectron spectroscopy results of MOFs after three cycles of photocatalysis. *Left*: Before photocatalysis (red) and after photocatalysis (yellow) of UiO-66-CrCAT. *Right*: Before photocatalysis (green) and after photocatalysis (cyan) of UiO-66-GaCAT. The oxidation state of metal ions was unchanged during 18 hours of photocatalysis.

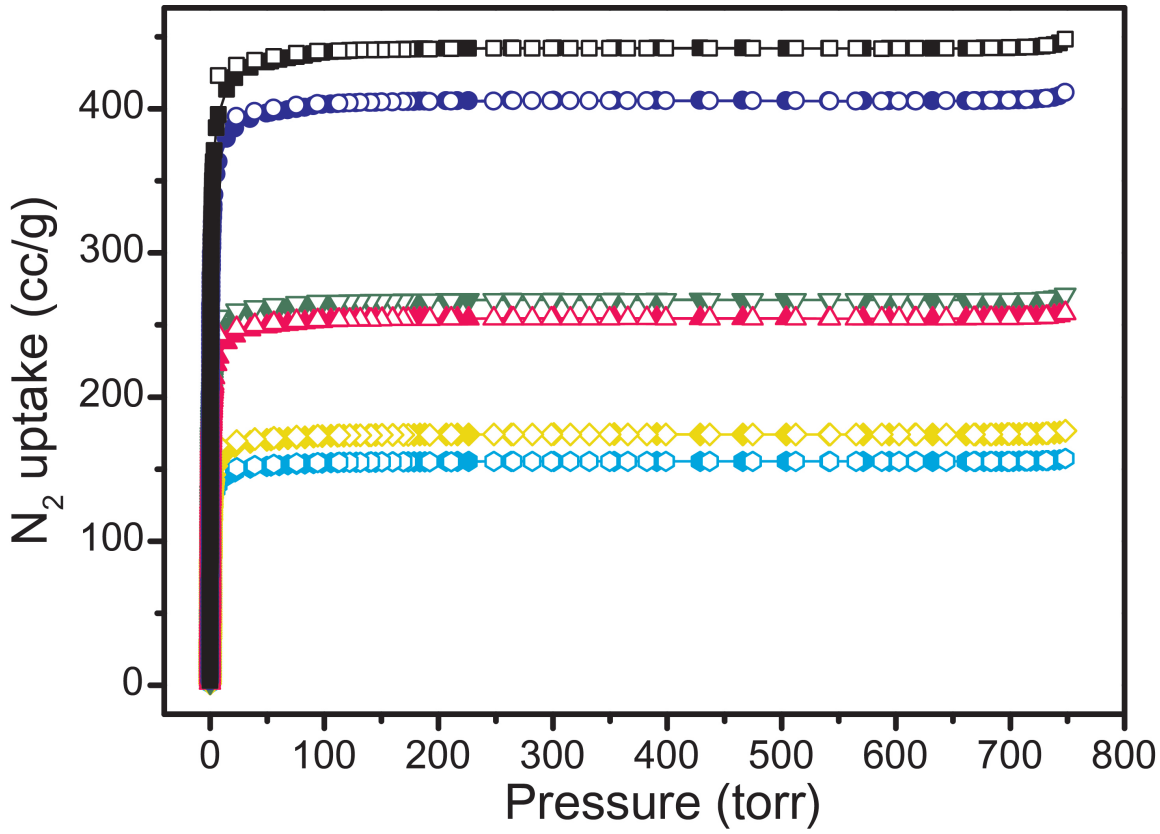

Fig. S10. N_2 isotherms of MOF samples prepared in the study. The filled shapes represent adsorption and open shapes represent desorption, respectively. Black squares = UiO-66; blue circles = UiO-66-CAT; pink triangles = UiO-66-CrCAT; green triangles = UiO-66-GaCAT; yellow diamonds = UiO-66-CrCAT after three photocatalysis cycles; and cyan hexagons = UiO-66-GaCAT after three photocatalysis cycles. The specific surface area of UiO-66 was decreased after each postsynthetic modification due to additional elements to pristine UiO-66. It was found that the N_2 uptakes for both metalated MOFs were decreased after three cycles of photocatalysis and this indicates some pores were blocked or collapsed during photocatalysis.

	Initial	After 1 cycle	After 2 cycle	After 3 cycle
UiO-66-CrCAT	0.25	0.238	0.223	0.209
UiO-66-GaCAT	0.26	0.249	0.227	0.203

Table S1. M(III)/Zr(IV) ratio in UiO-66-M(III)CAT MOFs after each cycle of photocatalysis.

	UiO-66-CrCAT	UiO-66-GaCAT	UiO-66-FeCAT	UiO-66-CAT
TON	11.22	6.14	0.34	0

Table S2. Turnover numbers for UiO-66 derivatives for photocatalytic CO_2 reduction. All samples were placed in 0.1M BNAH 4:1 MeCN-TEOA solution with visible light irradiation for 6 h.

	a_1	τ_1 (ns)	a_2	τ_2 (ns)	τ_{ave} (ns)
UiO-66-CAT	0.01	0.67	0.99	0.12	0.15
UiO-66-CrCAT	0.11	1.36	0.89	0.24	0.70
UiO-66-GaCAT	0.20	0.72	0.80	0.18	0.45

Table S3. Lifetime values of solid-state fluorescence in UiO-66-CAT series using a 375 nm laser.

Name	Photosensitizer	Solvent	TOF (h^{-1})	Reference
InP	Ru(4,4'-diphosphate ethyl-2,2'-bipyridine)$(CO)_2Cl_2$	Water	0.12	*J. Am. Chem. Soc.* **2011**, 133, 15240
InP	Ru(4,4'-di(1*H*-pyrrolyl-3-propyl carbonate)-2,2'-bipyridine}$(CO)(MeCN)Cl_2$]	Water	0.33	*J. Am. Chem. Soc.* **2011**, 133, 15240
ZnS	None (UV light)	Water Isopropanol	0.02	*Appl. Catal. B* **2015**, *online*
N doped Ta_2O_5	$Ru(bpy)_2(CO)_2$	MeCN/TEOA	0.32	*Chem. Commun.* **2011**, 47, 8673
C-$LaCo_{0.95}Fe_{0.05}O_3$	None	$Na_2CO_{3(aq)}$	0.03	*Catal. Commun.* **2009**, 11, 87
MWCNT/TiO_2	None (UV light)	Water	0.002	*Carbon* **2007**, 45, 717
UiO-66-Cr(III)CAT	None	MeCN/TEOA BNAH	1.87	This work
UiO-66-Ga(III)CAT	None	MeCN/TEOA BNAH	1.02	This work

Table S4. Photocatalytic ability of MOFs compared to non-MOF, heterogeneous systems for the reduction of CO_2 to $HCOO^-$ or HCOOH. UiO-66-M(III)CAT showed much higher TOF values when compared to various heterogeneous systems.

Name	Photosensitizer	Solvent	TOF (h^{-1})	Reference
$[Ru(bpy)_2(CO)_2](PF_6)_2$	$[Ru(bpy)_3](PF_6)_2$	DMF/Water BNAH	56	*Inorg. Chem.* **2014**, *53*, 3326
$[\{(dmb_2)Ru(bpyC_2bpy)\}_2$ $Ru(CO)_2](PF_6)_6$	None	DMF/TEOA BNAH	28	*PNAS* **2012**, *109*, 15673
fac-$Mn(bpy)(CO)_3Br$	$[Ru(bpy)_3]^{2+}$	DMF/TEOA BNAH	13	*Chem. Commun.* **2014**, *50*, 1491
cis,trans-$[Ru\{4,4'-(CH_2PO_3H_2)_2$- 2,2'-bpy$\}(CO)_2Cl_2]$	g-C_3N_4	MeCN/TEOA	10	*Chem.Commun.* **2013**, *49*, 10127
$[Ru(bpy)_2(MebpyCH_2CH_2(bpy)$ $Me)Re(CO)_3Cl]Cl_2 \bullet 8H_2O$	None	H_2O Ascorbate	1.04	*Inorg. Chem.* **2015**, 54, 1800
UiO-66-Cr(III)CAT	None	MeCN/TEOA BNAH	1.87	This work
UiO-66-Ga(III)CAT	None	MeCN/TEOA BNAH	1.02	This work

Table S5. Photocatalytic ability of MOFs compared to homogeneous systems for the reduction of CO_2 to HCOOH or formate. UiO-66-M(III)CAT showed lower TOF values when compared to various homogeneous systems. However, the MOF photocatalysts were robust, recyclable, and unlike most homogeneous photocatalytic systems did not require an exogenous photosensitizer.

Name	Photosensitizer	Solvent	TOF (h^{-1})	Reference
MOF-253-Ru$(CO)_2Cl_2$	None	MeCN/TEOA	0.363	*Chem. Commun.* **2015**, 51, 2645
NH_2-MIL-101(Fe)	None	MeCN/TEOA	0.05	*ACS Catal.* **2014**, 4 4254
NH_2-MIL-53(Fe)	None	MeCN/TEOA	0.013	*ACS Catal.* **2014**, 4 4254
NH_2-MIL-88B(Fe)	None	MeCN/TEOA	0.008	*ACS Catal.* **2014**, 4 4254
Y-Ir(bpy)$(ppy)_2(COOH)_2$	None	MeCN/TEOA	0.095	*Chem. Sci.* **2014**, *5*, 3808
NH_2-MIL-125(Ti)	None	MeCN/TEOA	0.044	*Angew. Chem. Int. Ed.* **2012**, 51, 3364
NH_2-MIL-125(Ti)	None	MeCN/TEOA BNAH	0.253	*Chem. Commun.* **2015**, 51, 5735
$Zr_{4.3}Ti_{1.7}O_4(OH)_4(NH_2bdc)_{5.17}((NH_2)_2bdc)_{0.83}$	None	MeCN/TEOA BNAH	1.04	*Chem. Commun.* **2015**, 51, 5735
UiO-66-Cr(III)CAT	None	MeCN/TEOA BNAH	1.87	This work
UiO-66-Ga(III)CAT	None	MeCN/TEOA BNAH	1.02	This work

Table S6. Photocatalytic ability of CAT MOFs compared to other MOF-based photocatalytic systems that have been reported. UiO-66-M(III)CATs showed comparable TOF number than MOF photocatalytic systems.